Regular Article

The structure of clusters formed by Stockmayer supracolloidal magnetic polymers

Ekaterina V. Novak[1], Elena S. Pyanzina[1], Pedro A. Sánchez[1,2], and Sofia S. Kantorovich[1,3,a]

[1] Ural Federal University, Lenin Av. 51, 620000, Ekaterinburg, Russia
[2] Helmholz-Zentrum Dresden-Rosendorf, Bautzner Landstrasse 400, 01328 Dresden, Germany
[3] University of Vienna, Sensengasse 8, 1090, Vienna, Austria

Abstract. Unlike Stockmayer fluids, that prove to undergo gas-liquid transition on cooling, the system of dipolar hard or soft spheres without any additional central attraction so far has not been shown to have a critical point. Instead, in the latter, one observes diverse self-assembly scenarios. Crosslinking dipolar soft spheres into supracolloidal magnetic polymer-like structures (SMPs) changes the self-assembly behaviour. Moreover, aggregation in systems of SMPs strongly depends on the constituent topology. For Y- and X-shaped SMPs, under the same conditions in which dipolar hard spheres would form chains, the formation of very large loose gel-like clusters was observed (E. Novak *et al.*, J. Mol. Liq. **271**, 631 (2018)). In this work, using molecular dynamics simulations, we investigate the self-assembly in suspensions of four topologically different SMPs —chains, rings, X and Y— whose monomers interact via Stockmayer potential. As expected, compact drop-like clusters are formed by SMPs in all cases if the central isotropic attraction is introduced, however, their shape and internal structure turn out to depend on the SMPs topology.

1 Introduction

Dipolar interactions alone do not seem to lead to the classical vapour-liquid phase transition in systems of spherical magnetic particles [1–9]. Instead, magnetic dipole-dipole interaction is responsible for extensive self-assembly phenomena. Thorough investigations of dipolar systems carried out for more than 30 years showed that the most probable cluster topologies observed in dipolar hard sphere systems are chains, rings, Y- and X-junctions [10–12]. As temperature decreases and concentration increases, those structures of magnetic particles form loose networks [8,13].

Modern experimental techniques allow the stabilisation of dipolar clusters by polymer crosslinking, forming supracolloidal magnetic polymer-like structures [14–17]. In general, the behaviour of chain-like magnetic SMPs has been actively investigated in experiment [18–21], theory [22–24] and coarse-grained computer simulations [25–28]. All these works agree that SMPs represent a promise for potential medical and microfluidics application [29,30]. In a recent study, we generalised the analysis of SMPs to the rest of basic structures formed by self-assembly of dipolar spheres [31, 32]. The interest to study rings-, X- and Y-like SMPs is twofold. First, once synthesised, such structures can be useful building blocks for novel magnetic soft materials. Second, they offer a new approach to

the theoretical study of self-assembled structures. *In silico* investigations [32] showed basically no self-assembly in suspensions of ring-shaped SMPs; chain-like SMPs formed linear clusters, whose size distribution exhibited an exponential decay. In contrast, Y and X SMPs form very large but rather loose clusters with up to 90 per cent of system SMPs connected in them. Such clusters can be considered as precursors for a phase transition. These results agree well with the phase behaviour observed for patchy particles of different valency [33], where the authors show that the gas-liquid critical point shifts towards lower temperature if the valency decreases. In fact, linear SMPs can be associated with the patchy particles of valency two, whereas Y- and X-like SMPs exhibit a behaviour analogous to patchy particles with valency three and four, respectively.

Another actively studied system whose behaviour is largely defined by dipole-dipole interactions is the Stockmayer fluid. Additionally to dipolar forces, Stockmayer particles experience a short-range isotropic attraction. The properties of these systems were investigated in detail by many authors and it was found that a Stockmayer fluid undergoes a vapour-liquid phase transition on cooling and when concentration increases [34–38]. Thus, colloidal particles form compact isotropic clusters.

The idea of the present study is to combine our knowledge about self-assembly of SMPs and Stockmayer flu-

[a] e-mail: sofia.kantorovich@univie.ac.at

ids and elucidate the self-assembly of SMPs of different topologies, when magnetic particles (SMP monomers) composing them experience an additional central attraction.

The structure of the manuscript is the following. First, we introduce the model and describe methods. When discussing results, we start with discussing macroscopic characteristics, such as cluster size distributions and cluster shape description. In order to explain the differences brought up by topology into the cluster shape, as the next step, we study the structure of clusters and report the orientation of individual SMPs, as well as their dipole moments in the cluster. Next, we go down to the particle (monomer) resolution and analyse the neighbourhoods of monomers in the cluster and monomer dipolar orientations. Finally, we compare the properties of the clusters formed by SMPs to those found in a non-crosslinked Stockmayer fluid.

2 Model and simulation details

For modelling a dispersion of SMPs, we used a bead-spring model with a system of reduced units. We assume that a SMP consists of monodisperse ferromagnetic spherical particles of diameter $\sigma = 1$ and mass $m = 1$, with a permanent magnetic moment represented by a point dipole, $\vec{\mu}$, placed in the particle centre. The long-range magnetic interaction between any pair i, j of magnetic particles (SMP monomers) is described by the dipole-dipole potential:

$$U_{dd}(\vec{r}_{ij}) = \frac{\vec{\mu}_i \cdot \vec{\mu}_j}{r^3} - \frac{3[\vec{\mu}_i \cdot \vec{r}_{ij}][\vec{\mu}_j \cdot \vec{r}_{ij}]}{r^5}, \qquad (1)$$

where $\vec{\mu}_i$ and $\vec{\mu}_j$ are their respective dipole moments, $\vec{r}_{ij} = \vec{r}_i - \vec{r}_j$ is the displacement vector connecting their centres and $r = |\vec{r}_{ij}|$.

To model the central attraction between the monomers of SMPs, a Lennard-Jones potential is used that, considering $\sigma = 1$ and setting the energy scale to unity, can be written as

$$U_{\mathrm{LJ}}(r) = 4\left(r^{-12} - r^{-6}\right). \qquad (2)$$

The bonding between crosslinked monomers within every polymer is modelled as a pair potential with two terms. The first term is a simple harmonic spring whose ends are attached to the monomer surfaces, as shown in fig. 1(a). The spring attachment points are placed at the projection points of the head and the tail of the central dipole moment. The second term corresponds to a FENE potential that limits the maximum extension of the bond. Therefore, the bonding potential is defined as

$$U_S(\vec{r}_{ij}) = \frac{K}{2}\left[\left(\vec{r}_{ij} - \frac{1}{2}(\hat{\mu}_i + \hat{\mu}_j)\right)^2 - \frac{r_0^2}{2}\ln\left[1 - \left(\frac{\vec{r}_{ij}}{r_0}\right)^2\right]\right], \qquad (3)$$

where K is the energy scale of the interaction, $\hat{\mu}_i = \vec{\mu}_i/|\vec{\mu}_i|$ and $\hat{\mu}_j = \vec{\mu}_j/|\vec{\mu}_j|$ are the unitary vectors parallel to each associated dipole moment and r_0 is the maximum allowed extension for the bond. We take $K = 30$ and
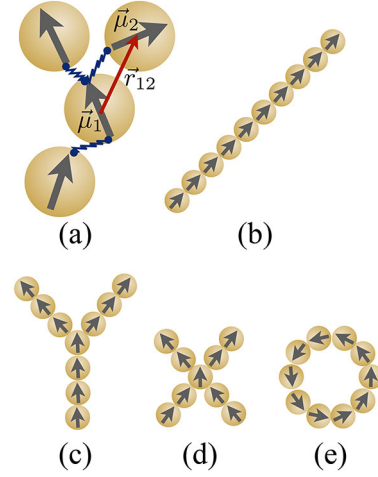

Fig. 1. Explanation of the model. (a) Crosslinking and magnetic moments. (b) Chain-like SMPs; (c) Y-like SMPs; (d) X-like SMPs; (e) ring-like SMPs.

$r_0 = 1.5$ in reduced units in accordance with our previous studies [31,39].

We performed molecular dynamics simulations in the canonical ensemble, using a Langevin thermostat in order to approximate implicitly the effects of the thermal fluctuations of the background fluid. Periodic boundary conditions were used. The simulations were performed in the ESPResSo 3.2.0 package [40]. The initial simulation box contained 512 identical magnetic polymers with size either $L = 10$ for chain-like, Y-like and ring-like SMPs or $L = 9$ for X-structures in their basic configurations as shown in fig. 1(b)–(e). The dimensionless reduced concentration of monomers was always fixed to $\rho^* = N\sigma/V = 0.05$, where the number of monomers, N, and the volume of the simulation box, V, are identical for all but X-like SMPs. SMPs were initially placed parallel to each other at random positions. The magnetic moment of each monomer μ in dimensionless units was fixed so that $\mu^2 = 5$. The system was first equilibrated at high $T = 4$ to assure random initial configuration before switching on magnetic interactions and central attraction. Afterwards, before the production runs were performed, the system was re-equilibrated at $T = 1$ for $9 \cdot 10^5$ integration steps, using a time step $\delta t = 5 \cdot 10^{-3}$. After this re-equilibration cycle, we checked that all sampled systems already reached a stationary state, in which energy only fluctuates around a constant value. Finally, a production cycle of $3 \cdot 10^6$ steps was performed, in which the system configurations were measured at intervals of 10^5 steps. The long-range magnetic interactions were calculated using the dipolar-P^{3}M algorithm [41].

A typical simulation snapshot during the production is presented in fig. 2. This very snapshot is taken from the system of Y-like SMPs, but it is impossible to visually spot the difference between the snapshots taken from other suspensions. It can be seen that the system is composed by quasi-spherical aggregates containing multiple SMPs. Besides this apparent overall resemblance, we want to determine whether the clusters have the same internal
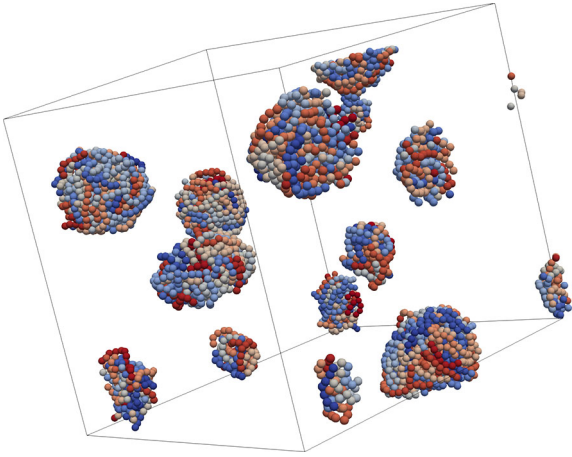
Fig. 2. Typical simulation snapshot. Clusters formed by Y-like SMPs. Different colours help to distinguish different SMPs.

structure independently of the SMPs topology. For this we performed a systematic cluster analysis of the obtained aggregates. In all cases we identify the non-permanent connections between the monomers by means of a combination of distance or distance and energy criteria. In both cases the two monomers are considered to be connected if their centre-to-centre distance is smaller than $r_{ij} \leq 2^{1/6}$; in the second case, additionally their dipole-dipole pair energy, given by expression (1), $U_{dd}(\vec{r}_{cut}; \vec{\mu}_1, \vec{\mu}_2) < 0$, should be negative.

3 Results and discussions

In order to thoroughly investigate the internal structure of the clusters we will increase the resolution step by step from individual clusters, through SMPs within them to monomers. In other words, first, the cluster shapes for each SMP topology will be analysed. Next, we will study the orientation and positioning of individual SMPs within clusters and the orientations of their magnetic moments. Finally, going to the individual particle level, we will elucidate the neighbourhoods of monomers and the orientations of their dipole moments within the clusters.

3.1 Cluster distributions and shapes

The size-distribution of clusters formed by chain-like SMPs ranges between 20 and 300 SMPs per cluster, with the maximum around 30. The clusters made of other SMP topologies have size distributions that are narrower than for the case of chains and all of them range between 10 and 140. The maxima of the cluster size distributions, in case of Y-, X- and ring-like SMPs, occur in the same region as for clusters formed by chain-like SMPs, around 30. It is worth noting that below all results are obtained through averaging over all clusters independently of their size. Such an approach is validated not only by the increased statistics, but also by the following fact: the comparison between the aforementioned averaging procedure

and the averaging in which only overlapping size regions near distribution maxima (between 20 and 50 for all SMPs topologies), does not reveal any qualitative changes in the results.

As discussed above, visual inspection of fig. 2 does not reveal any differences between clusters formed by different SMPs. Zoomed-in clusters with the size near the maximum of the distribution are shown in fig. 3 that consists of four columns. Each column corresponds to the topology of cluster-forming SMPs. In the upper row all monomers in the clusters are depicted as solid spheres, whereas in the lower row we see only several selected SMPs while all other monomers are transparent and are only represented by their dipole moments. Looking at these clusters in the upper row and taking into account that all four of them are composed by approximately the same number of SMPs it seems that they have a slightly different shape. In order to quantify these differences we calculate two shape descriptors: the asphericity and the relative shape anisotropy. The asphericity b is defined by

$$b = \lambda_3^2 - \frac{1}{2}\left(\lambda_1^2 + \lambda_2^2\right), \qquad (4)$$

where $\lambda_{1(2,3)}$ are the eigenvalues of the gyration tensor of the cluster. Parameter $b = 0$ if the distribution of particles is spherically symmetric. In fig. 4 we plot the histograms that show the fraction of clusters formed by each SMP topology with a given value of b. Clearly, none of the formed clusters is perfectly spherical. The histograms which exhibit maximum close to zero are those for X- and Y-shaped SMP clusters as seen in figs. 4(c) and (b), respectively. The histogram for clusters formed by chain-like SMPs (fig. 4(a)) has a clear maximum at $b = 2$ and a secondary maximum around 5. There are basically no clusters formed by chain-like SMPs with $b > 7$. It is different for clusters formed by SMPs of any other topology: one can find several clusters with asphericity up to 12. The broadest distribution and the lowest sphericity can be found for clusters formed by ring-like SMPs, as shown in fig. 4(d).

In order to shed more light on the shape of SMPs clusters we look at their relative shape anisotropy κ^2. It is defined as

$$\kappa^2 = \frac{3}{2}\frac{\lambda_1^4 + \lambda_2^4 + \lambda_3^4}{(\lambda_1^2 + \lambda_2^2 + \lambda_3^2)^2} - \frac{1}{2}, \qquad (5)$$

and it is bounded between zero and one. $\kappa^2 = 0$ only occurs if all particles are distributed spherically symmetric with respect to the centre of mass of the cluster, and $\kappa^2 = 1$ only occurs if all particles lie on a line. We plot the resulting histograms in fig. 5. From all four subfigures one can immediately conclude that none of the clusters shows a tendency to elongate. As it can be seen, for clusters formed by chain-like SMPs (fig. 5(a)), the anisotropy shows the narrowest distribution with a clearly pronounced maximum for values $0.04 < \kappa^2 < 0.06$. For clusters formed by Y-like SMPs, shown in fig. 5(b) the maximum of the distribution is situated in nearly the same place, however the distribution seems to be broader. We find a rather broad distribution also for clusters formed
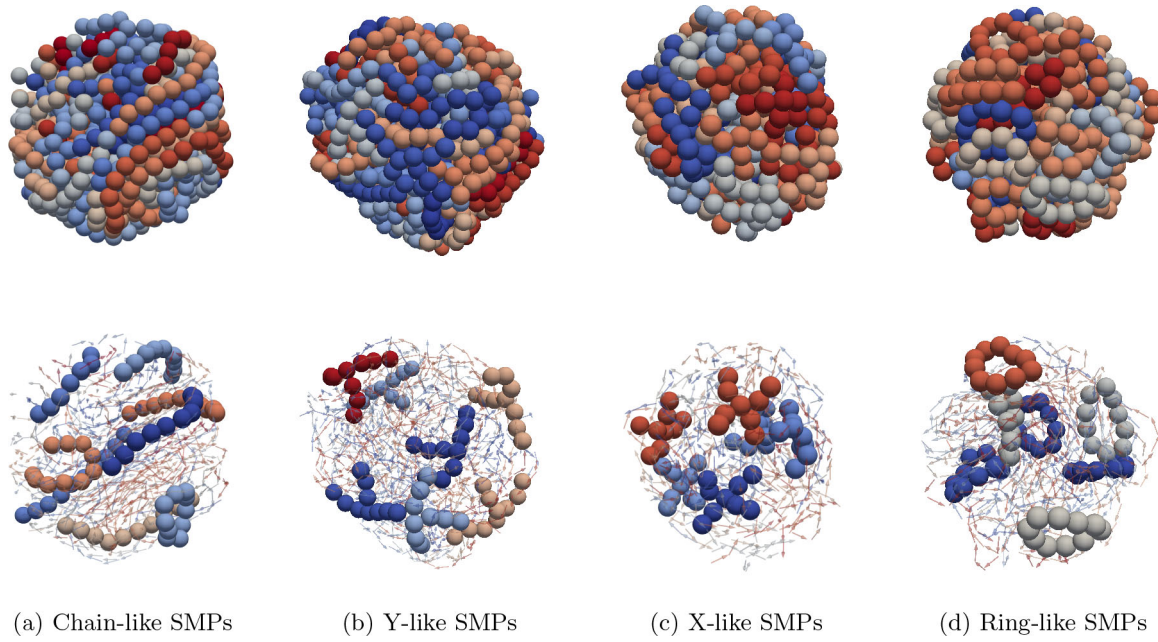
(a) Chain-like SMPs   (b) Y-like SMPs   (c) X-like SMPs   (d) Ring-like SMPs

Fig. 3. Snapshots of typical clusters. In the upper row all monomers are shown, whereas in the lower row only selected SMPs are visualised, the rest of the monomers are represented by arrows of their dipoles. Columns: (a) chain-like SMPs; (b) Y-like SMPs; (c) X-like SMPs; (d) ring-like SMPs.
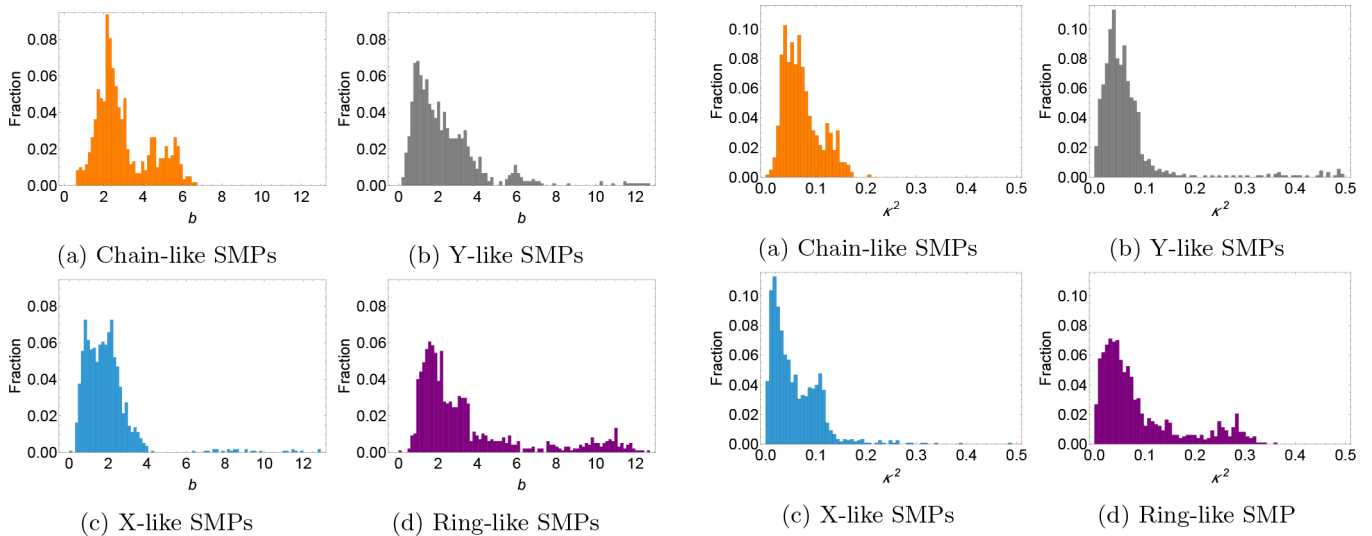

(a) Chain-like SMPs   (b) Y-like SMPs

(c) X-like SMPs   (d) Ring-like SMPs

Fig. 4. Histograms showing the fraction of clusters with a given asphericity b calculated from (4). The values are averaged over all production runs. Subfigures are for clusters formed by (a) chain-like SMPs; (b) Y-like SMPs; (c) X-like SMPs and (d) by ring-like SMPs.

(a) Chain-like SMPs   (b) Y-like SMPs

(c) X-like SMPs   (d) Ring-like SMP

Fig. 5. Histograms showing the fraction of clusters with a given anisotropy κ^2 calculated from (5). The values are averaged over all production runs. Subfigures are for clusters formed by (a) chain-like SMPs; (b) Y-like SMPs; (c) X-like SMPs and (d) by ring-like SMPs.

by X-like and ring-like SMPs (figs. 5(c) and (d)), though with one difference: the distribution for clusters of ring-like SMPs is almost bimodal. The latter agrees well with the distribution of asphericity provided in fig. 4(d), where one can find a fraction of clusters whose asphericity is $10 < b < 13$.

So far, the outcome of our analysis can be summarised as follows. There are differences in the overall shape of

clusters formed by SMPs with different topology. The differences are not large, but still significant. Moreover, the largest similarities are observed between clusters formed by Y-like and X-like SMPs, whereas those formed by chains and rings have clearly different shape characteristics. The next step is to explain observed features and look inside different clusters.
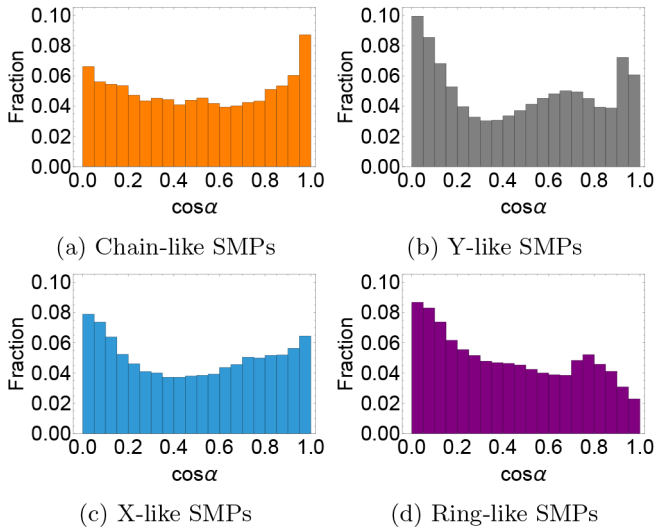
Fig. 6. Fraction of SMPs, whose main axis and the vector, connecting the centre of mass of the cluster and that of an SMP, form $\cos\alpha$. The values are averaged over all production runs. Subfigures are for clusters formed by (a) chain-like SMPs; (b) Y-like SMPs; (c) X-like SMPs and (d) by ring-like SMPs.

Fig. 7. Fraction of SMPs, whose magnetic moment $\vec{M}$, defined in eq. (6), and the vector, connecting the centre of mass of cluster and that of an SMP, form $\cos\beta$. The values are averaged over all production runs. Subfigures are for clusters formed by (a) chain-like SMPs; (b) Y-like SMPs; (c) X-like SMPs and (d) by ring-like SMPs.

3.2 Clusters inside: SMP level

First we address the orientation of SMPs within the clusters. Let us calculate the main axis of a SMP inside a cluster. It can be obtained as the eigenvector corresponding to the largest eigenvalue of the SMP gyration tensor. The next step is to calculate the vector, connecting the centre of mass of the cluster to that of a SMP. After that, one can define the angle α between the latter vector and SMP main axis. The average value of this angle will characterise different orientations of SMPs within the clusters. In case the structure of the cluster is onion-like, aforementioned angle α should be close to $\pi/2$, *i.e.* the major part of SMPs is oriented tangentially. On the other hand, if $\alpha \sim 0$, it means that SMPs are oriented radially. In fig. 6, we plot the fraction of SMPs with a given topology as a function of $\cos\alpha$. The plots are symmetric with respect to zero, that is why we show the data from 0 to 1. It is rather surprising that obtained distributions exhibit much clearer differences depending on the topology in comparison to shape characteristics studied in the previous section. It turns out that the chain-like SMPs (fig. 6(a)) can have practically any orientation inside the clusters with only mild preference to radial orientation. This finding clearly indicates that chain-like SMPs do not form onion-like clusters. Actually, the only clusters that have an onion-like structures are those formed by rings. The distribution in fig. 6(d) is the only one that shows no maximum at $\cos\alpha = 1$. From figs. 6(b) and (c) we can conclude that both Y-like and X-like SMPs with higher probability form onion-like clusters, however, there can be also seen the secondary maximum corresponding to radial orientation. With this information at hand, visual examination of the lower row of fig. 3 can reveal the same tendency: the clusters formed by ring-like SMPs have an onion internal structure, whereas X- and
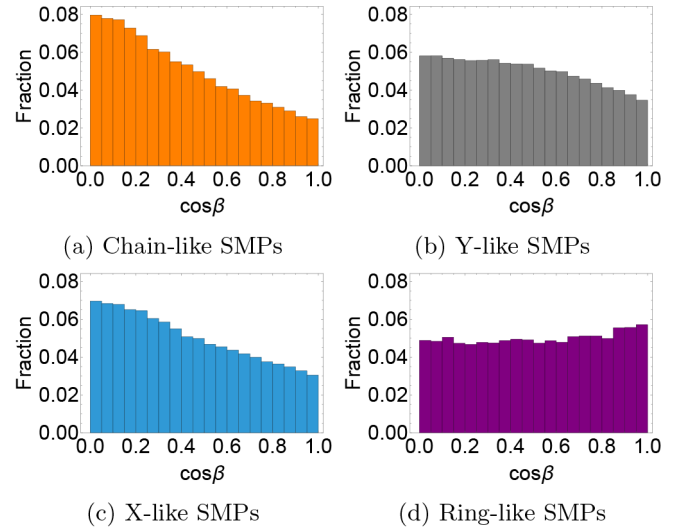
Y-like SMPs have mixed orientations with light preference towards tangential orientation. Most uniform orientation distribution can be found inside clusters formed by chain-like SMPs.

Another interesting question is whether the orientation of an SMP inside the cluster is correlated with the orientation of its total dipole moment. So, as a second step, we computed the relative net magnetic moment of each SMP, $\vec{M}$, according to

$$\vec{M} = \frac{1}{L\mu} \sum_{i=1}^{L} \vec{\mu}_i. \qquad (6)$$

Analogously to α, one can define angle β between $\vec{M}$ of an SMP and the vector, connecting centres of mass of cluster and current SMP. In fig. 7 we plot the fraction of SMPs, whose magnetic moment forms angle β with the vector connecting its centre of mass and the centre of mass of a cluster. Similar to fig. 6, here maximum at unity means the predominance of the radial orientation of $\vec{M}$ inside the cluster, whereas maximum at zero means the predominance of tangential orientation. Interestingly enough, figs. 7(a)–(c) show that the orientation only weakly depends on the topology of SMPs: all the distributions monotonically decrease with growing $\cos\beta$, albeit for clusters made of Y-like SMPs the decay is weaker than for the others. The only uniform distribution of the dipole moment orientation can be found inside cluster made by ring-like SMPs, as seen in fig. 7(d). However, one should keep in mind that the net dipole moment of a ring-like SMP is close to zero. As a result, one would not expect any kind of correlations between net dipoles of ring-like SMPs.
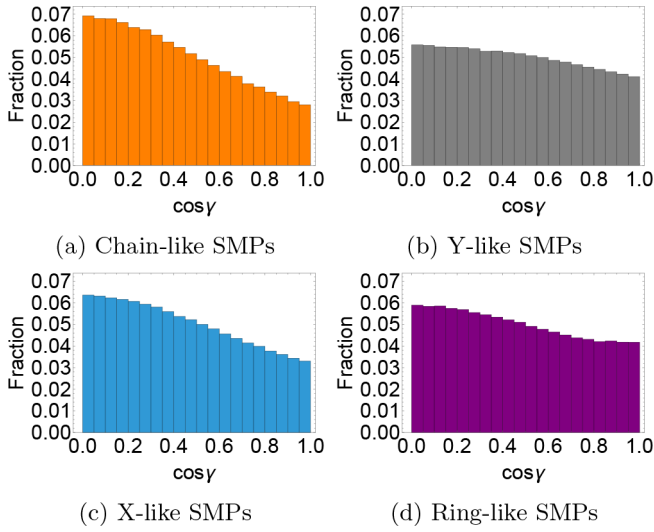
Fig. 8. Fraction of monomers, whose magnetic moment $\vec{\mu}$ and the vector, connecting the centre of mass of the cluster and that of an SMP, form $\cos\gamma$. The values are averaged over all production runs. Subfigures are for clusters formed by (a) chain-like SMPs; (b) Y-like SMPs; (c) X-like SMPs and (d) by ring-like SMPs.

Fig. 9. Histogram of the total amount of non-permanent neighbours that each monomer has in a cluster. No discrimination is made: both monomers from the same SMP and from different ones are counted. The values are averaged over all production runs. Subfigures are for clusters formed by (a) chain-like SMPs; (b) Y-like SMPs; (c) X-like SMPs and (d) by ring-like SMPs.

Summarising this part of the analysis, we can say that the internal orientation of the SMPs in the formed clusters depends on their topology. Chain-like SMPs interlace and can have basically a random orientation inside the cluster, with high probability they can penetrate from surface to the centre of the cluster radially or as well oriented tangentially to the cluster surface. The rings, instead, do not mix and form clusters with onion structure and it is rather rare to find a ring oriented with its main axis radially inside the cluster. Y-like and X-like SMPs also have a preference to be tangential to the cluster surface, however both topologies might also acquire radial orientation. The orientation of the net SMP dipole moment in clusters formed by all but ring-like SMPs is predominantly tangential and the probability of an orientation decreases monotonically, approaching the radial one. We find that for chain-, Y- and X-like SMPs, the probability of their dipoles to be oriented radially is at least twice lower than that of a tangential one. As for ring-like SMPs, their net dipole moment is infinitesimally small, as a result we find no preferred orientation of $\vec{M}$ in this case.

3.3 Clusters inside: monomer level

After having investigated the orientations of SMPs net magnetic moments, we look at individually magnetic moments $\vec{\mu}$ of monomers inside the clusters. In order to do that, for each monomer, we calculated the angle, γ, between $\vec{\mu}$ and the vector connecting the centre of the monomer to the centre of mass of the cluster. The results are presented in fig. 8. Here, it becomes clear that independently of the SMP topology, monomers in them have a preference to orient tangentially inside the clusters. This is an outcome of the optimisation of dipolar interactions.
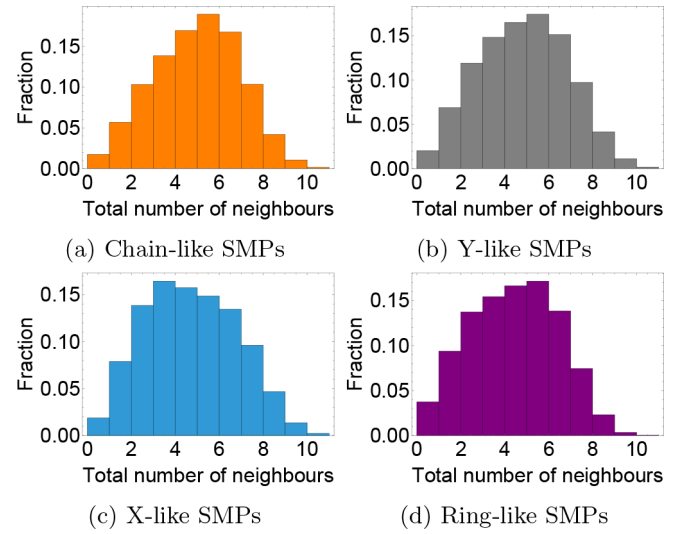
Topology of an SMP can slightly enhance or inhibit the tendency to be oriented tangentially. Thus, for chain-like SMPs shown in fig. 8(a), the ratio between the fraction of monomers oriented tangentially and radially is larger than two, for monomers in X-like SMPs this ratio is slightly smaller than two (fig. 8(c)). If one calculates the same ratio for monomers in Y-like and ring-like SMPs (figs. 8(b) and (d), respectively) it will be around 40 per cent, *i.e.* much smaller than for other two topologies.

Turning again to the lower row in fig. 3, one can now indeed notice that the dipoles form vortexes.

As indicated by fig. 9, where we plot the fractions of monomers with a given number of nearest neighbours, on the level of monomers all clusters are relatively dense. Light asymmetry of the plots does not affect the main conclusion. In order to understand if monomers in various SMPs in the clusters are mainly connected to monomers from different SMPs or to monomers of the SMP they belong to, we calculated how many non-permanent bonds inside one SMP can be found. In other words, for each monomer, we calculated how many neighbours it has that belong to the same SMP and are not precrosslinked ones. The results are shown in fig. 10. Here, one can notice again the influence of SMP topology. Thus, monomers in chain-like SMPs, see fig. 10(a), are not likely to have non-permanent neighbours within one SMP, whereas for Y-, X- and ring-like SMPs (figs. 10(b)–(d)), the probability of self-touching is higher, albeit still not significant. The fraction of such neighbours point to low degree of SMP folding inside the clusters, that is the result of the dipolar forces that favour head-to-tail orientations of monomer dipoles and the coupling between dipolar orientation with the structure backbone. The most likely to have self-contacts
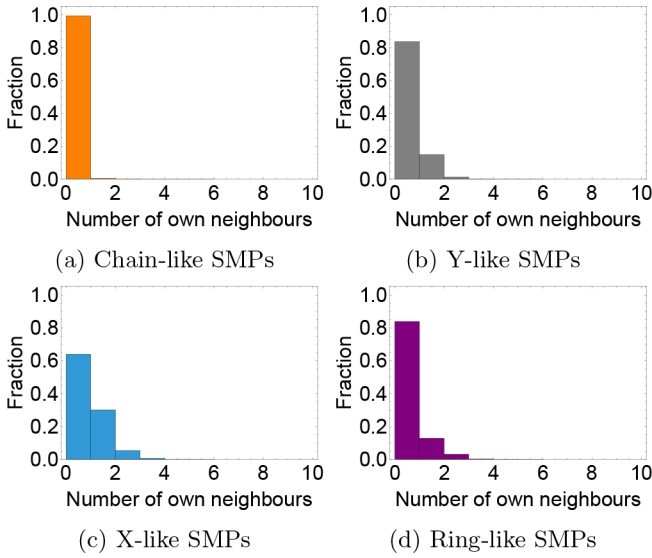
Fig. 10. Histogram of the total amount of non-permanent neighbours from the same SMP that a monomer in the cluster has. The values are averaged over all production runs. Subfigures are for clusters formed by (a) chain-like SMPs; (b) Y-like SMPs; (c) X-like SMPs and (d) by ring-like SMPs.

are X-like SMPs due to the fact that they have the shortest arms and the highest induced monomer proximity by design.

In order to quantitatively characterise spatial monomer distribution and rule out the possibility of crystallisation, we calculated the order parameters for all clusters and SMPs topologies:

$$Q_{lm}(\vec{r}) = Y_{lm}\left(\theta(\vec{r}), \phi(\vec{r})\right), \qquad (7)$$

where Y_{lm} are spherical harmonics of the respective order, lm, and angles θ and ϕ are respectively the azimuthal and polar angles of a bond between two neighbouring monomers inside the cluster, characterised by a vector $\vec{r}$, in a lab reference frame. The function $Q_{lm}(\vec{r})$ is averaged over all bonds in the cluster, then over all clusters and, finally, over all snapshots:

$$\overline{Q}_{lm} = \langle Q_{lm} \rangle. \qquad (8)$$

The resulting cumulant Q_l,

$$Q_l = \left[\frac{4\pi}{2l+1} \sum_{m=-l}^{l} |\overline{Q}_{lm}|^2 \right]^{1/2}, \qquad (9)$$

is plotted in fig. 11 in the form of histograms for all four SMPs topologies.

It is known that based on Q_l distribution, one can distinguish between different crystalline ordering in the system [42]. Looking at the histograms obtained for SMP clusters, we can safely conclude that they evidence no crystalline structure, as the values of Q_l are not only very low (below those found for supercooled Lennard-Jones liquid in ref. [42]), but also decay monotonically with l.
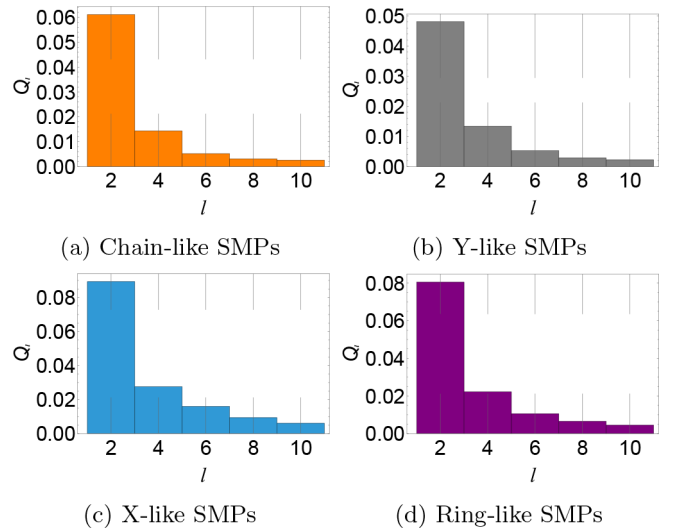

Fig. 11. Histograms of Q_l, eq. (9). The values are averaged over all production runs. Subfigures are for clusters formed by (a) chain-like SMPs; (b) Y-like SMPs; (c) X-like SMPs and (d) by ring-like SMPs.

Summarising this subsection we can say that on the monomer level the cluster structure is basically the same independently of the topology of the SMPs that form them. The only notable difference occurs on the level of SMP self-contacts inside the cluster, thus chain-like SMPs never self touch and so, the clusters will show the highest degree of mixing, whereas X-like SMPs are forming contacts inside themselves, thus presumably leading to less stable clusters, if any external force is to be applied.

3.4 Comparison to the Stockmayer fluid with non-crosslinked monomers

The final step in analysing the influence of permanent crosslinkers on the structure of clusters formed in Stockmayer systems, is to compare the properties of SMP clusters to that of non-crosslinked Stockmayer monomers. In order to make a fair comparison, we perform simulations of the Stockmayer system of independent monomers, whose size, dipole moment and volume fraction coincide with their counterparts in simulations of SMPs: $\sigma = 1$, $\mu^2 = 5$ and $\rho^* = 0.05$. Moreover, the simulations for this system were equally long as the simulations with SMPs. It is worth mentioning that with these parameters, the system corresponds to the metastable area of $T - \rho$-phase diagrams [35, 43]. Thus, the clusters we see, are indeed, only the precursors of phase separation.

In fig. 12, we present a characteristic snapshot of such clusters formed by non-crosslinked dipolar monomers. Even a visual comparison of this system to fig. 2 shows that the clusters are bigger and they are less. In fact, the number of the clusters decreases by the factor of two once the monomer crosslinkers were removed, whereas the size distribution lays between 100 and 2300 monomers, in comparison to Y-like SMPs, in which the largest observed
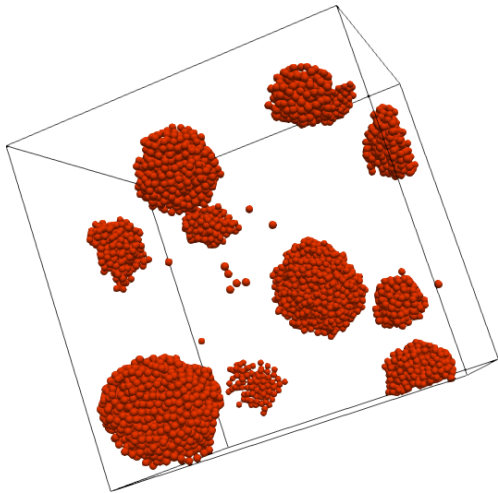
Fig. 12. Typical snapshot of a Stockmayer fluid, $\mu^2 = 5$; $\rho^* = 0.05$; $T = 1$; $\sigma = 1$.
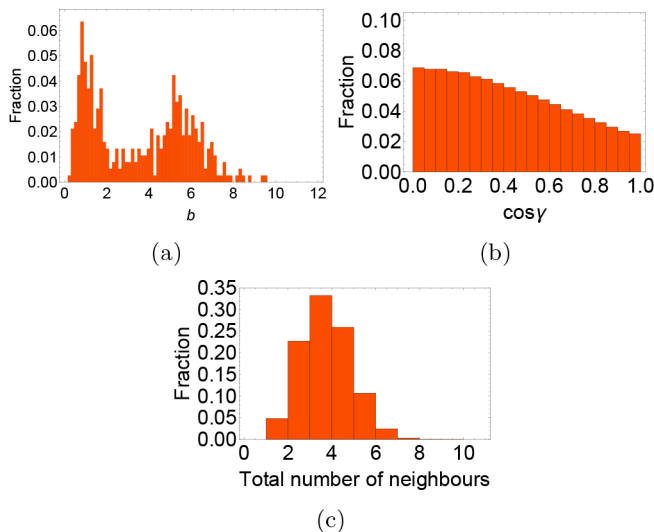

(a)

(b)

(c)

Fig. 13. For Stockmayer fluid (a) asphericity histogram (to be compared to fig. 4); (b) $\cos\gamma$ (to be compared to fig. 8); (c) the histogram of the total amount of nearest neighbours each monomer has (to be compared to fig. 9).

cluster contains 1430 monomers. As mentioned in sect. 1, the largest clusters observed in simulations of Stockmayer SMPs were found for chains: the biggest observed cluster contained 270 SMPs (2700 monomers), but all others had no more than 110 SMPs.

Looking at fig. 13, where, for the clusters formed in Stockmayer fluid, we plot the asphericity histogram in (a), the histogram for $\cos\gamma$ in (b) and the histogram of the total amount of nearest neighbours each monomer has in the cluster in (c), we notice the similarities in the properties of the monomers in the clusters here and of those in clusters formed by chain-like SMPs. Thus, for example, if one compares fig. 13(a) and fig. 4(a), the asphericity has two close but distinct maxima. On the other hand, the overwhelming tendency of monomers to align tangentially seem to be even stronger in a non-crosslinked state, com-

pare fig. 13(b) and fig. 8(a). Finally, the number of nearest neighbours each monomer has, fig. 13(c), shifts towards lower values in comparison to the histogram plotted in fig. 9(a): the absence of permanent crosslinkers results in overall loosening of the clusters.

To summarise this part, one can say that permanent crosslinkers lead to smaller and more compact clusters in Stockmayer systems, but do not prevent the monomers to orient tangentially inside the clusters.

4 Conclusion

In the present study we investigated the effect of the SMP topology on their self-assembly driven by anisotropic magnetic dipolar and central attraction interactions. The process of self-assembly in these systems, in contrast to non-crosslinked monomers, is a competition not only between the two aforementioned interactions, but also the result of a specific initial monomer crosslinking.

We show that the crosslinking does not change the main tendency of a Stockmayer fluid to phase separate. Thus, the overall shape of clusters weakly depends on the topology of the constituent SMPs. After having studied asphericity and anisotropy characteristics of the aggregates we found the following tendencies. All of them have a modest degree of anisometry. The lowest asymmetry is exhibited by clusters made of Y-like and X-like SMPs. The clusters formed by ring-like SMPs, in contrast, can assume a very broad range of shapes.

Increasing the resolution of the analysis, we studied the orientations of SMPs inside the clusters. It turned out that on this level the influence of the topology is the strongest. Chain-like SMPs mix with each other when forming clusters. This way, they might have almost any orientation inside the cluster. Ring-like SMPs, on the contrary, are preferably oriented tangentially to the cluster surface, thus, forming clusters with onion-like structure. Inside the clusters formed by Y-like and X-like SMPs one finds tangentially oriented building blocks with higher probability than radially oriented ones. However, the portion of SMPs with the latter orientation is not negligible. More uniformity is found when looking at the orientation of the net SMP magnetic moment: in case of clusters formed by chain-, Y- and X-like SMPs more than 60 per cent of the dipoles are oriented tangentially. The net magnetic moment of ring-like SMPs is a vanishing quantity, that is why their orientations are not well defined.

When focusing at monomers and their neighbourhood, we found that the SMPs that have more contacts with others are chain-like ones. The induced proximity of the monomers within X-like SMPs leads to the presence of bonds inside the same SMP, and as such slightly decreasing the overall number of non-permanent bonds a monomer forms in the cluster.

Finally, we compared the properties of clusters formed by different SMPs to those of clusters formed in a non-crosslinked Stockmayer fluid with the same dipolar strength and magnetic monomer concentration. These parameters correspond to a metastable state below the gas-

liquid critical point. It turns out that non-crosslinked monomers under the same conditions as SMPs form much larger clusters. However the alignment of magnetic moments in them is similar to that in the clusters formed by chain-like SMPs. In general, the shape of the clusters and the number of nearest neighbours each monomer has in them for the non-crosslinked system are similar to their counterparts for the system of chain-like SMPs. The latter has the lowest degree of crosslinking, thus, underlying the impact of SMPs topology.

The differences between the clusters formed by SMPs of different topology, observed in this study, will have an impact on the magnetic response of these systems. Moreover, the rheological properties, such as the behaviour of a cluster in a shear flow, will be also affected by the internal orientations of SMPs as well as the overall cluster anisotropy. These questions form the basis for our future investigations.

Author contribution statement

EVN performed the simulation and collected the data; ESP analysed the data and calculated structural properties; PAS developed simulation algorithms and crosslinking method for filaments of different topology; SSK posed the questions, took part in data analysis and wrote the main text of the manuscript.

References

1. R. van Roij, Phys. Rev. Lett. **76**, 3348 (1996).
2. R.P. Sear, Phys. Rev. Lett. **76**, 2310 (1996).
3. Y. Levin, Phys. Rev. Lett. **83**, 1159 (1999).
4. P.I.C. Teixeira, J.M. Tavares, M.M.T. da Gama, J. Phys.: Condens. Matter **12**, R411 (2000).
5. J.J. Weis, D. Levesque, Phys. Rev. Lett. **71**, 2729 (1993).
6. J.J. Weis, D. Levesque, Phys. Rev. E **48**, 3728 (1993).
7. T. Tlusty, S.A. Safran, Science **290**, 1328 (2000).
8. L. Rovigatti, J. Russo, F. Sciortino, Phys. Rev. Lett. **107**, 237801 (2011).
9. S. Kantorovich, A.O. Ivanov, L. Rovigatti, J.M. Tavares, F. Sciortino, Phys. Rev. Lett. **110**, 148306 (2013).
10. P.J. Camp, J.C. Shelley, G.N. Patey, Phys. Rev. Lett. **84**, 115 (2000).
11. M. Klokkenburg, R.P.A. Dullens, W.K. Kegel, B.H. Erné, A.P. Philipse, Phys. Rev. Lett. **96**, 037203 (2006).
12. M. Ronti, L. Rovigatti, J.M. Tavares, A.O. Ivanov, S.S. Kantorovich, F. Sciortino, Soft Matter **13**, 7870 (2017).
13. S.S. Kantorovich, A.O. Ivanov, L. Rovigatti, J.M. Tavares, F. Sciortino, Phys. Chem. Chem. Phys. **17**, 16601 (2015).
14. B.D. Korth, P. Keng, I. Shim, S.E. Bowles, C. Tang, T. Kowalewski, K.W. Nebesny, J. Pyun, J. Am. Chem. Soc. **128**, 6562 (2006).
15. P.Y. Keng, I. Shim, B.D. Korth, J.F. Douglas, J. Pyun, ACS Nano **1**, 279 (2007).
16. B. Bharti, A.-L. Fameau, M. Rubinstein, O.D. Velev, Nat. Mater. **14**, 1104 (2015).
17. H. Yuan, I.J. Zvonkina, A.M. Al-Enizi, A.A. Elzatahry, J. Pyun, A. Karim, ACS Appl. Mater. Interfaces **9**, 11290 (2017).
18. R. Dreyfus, J. Baudry, M.L. Roper, M. Fermigier, H.A. Stone, J. Bibette, Nature **437**, 862 (2005).
19. W.S. Choi, H.Y. Koo, J.Y. Kim, W.T.S. Huck, Adv. Mater. **20**, 4504 (2008).
20. K. Ērglis, D. Zhulenkovs, A. Sharipo, A. Cēbers, J. Phys.: Condens. Matter **20**, 204107 (2008).
21. F. Zhou, P.M. Biesheuvel, E.-Y. Choi, W. Shu, R. Poetes, U. Steiner, W.T.S. Huck, Nano Lett. **8**, 725 (2008).
22. A. Cēbers, Curr. Opin. Colloid Interface Sci. **10**, 167 (2005).
23. M. Belovs, A. Cēbers, Phys. Rev. E **79**, 051503 (2009).
24. I. Javaitis, V. Zilgalve, Adv. Mater. Res. **222**, 221 (2011).
25. P.A. Sánchez, J.J. Cerdà, V. Ballenegger, T. Sintes, O. Piro, C. Holm, Soft Matter **7**, 1809 (2011).
26. J.J. Cerdà, P.A. Sánchez, D. Lüsebrink, S.S. Kantorovich, T. Sintes, Phys. Chem. Chem. Phys. **18**, 12616 (2016).
27. J. Wei, F. Song, J. Dobnikar, Langmuir **32**, 9321 (2016).
28. A.A. Kuznetsov, J. Magn. & Magn. Mater. **470**, 28 (2019).
29. J. de Vicente, D.J. Klingenberg, R. Hidalgo-Alvarez, Soft Matter **7**, 3701 (2011).
30. B.J. Park, F.F. Fang, H.J. Choi, Soft Matter **6**, 5246 (2010).
31. D.A. Rozhkov, E.S. Pyanzina, E.V. Novak, J.J. Cerdà, T. Sintes, M. Ronti, P.A. Sánchez, S.S. Kantorovich, Mol. Simul. **44**, 507 (2018).
32. E. Novak, E. Pyanzina, D. Rozhkov, M. Ronti, J. Cerd, T. Sintes, P. Snchez, S. Kantorovich, J. Mol. Liq. **271**, 631 (2018).
33. E. Bianchi, R. Blaak, C.N. Likos, Phys. Chem. Chem. Phys. **13**, 6397 (2011).
34. B. Smit, C. Williams, E. Hendriks, S.D. Leeuw, Mol. Phys. **68**, 765 (1989).
35. M.E. van Leeuwen, B. Smit, Phys. Rev. Lett. **71**, 3991 (1993).
36. A.Z. Panagiotopoulos, Mol. Simul. **9**, 1 (1992).
37. M.J. Stevens, G.S. Grest, Phys. Rev. E **51**, 5962 (1995).
38. D. Adams, E. Adams, Mol. Phys. **42**, 907 (1981).
39. E. Novak, D. Rozhkov, P. Sánchez, S. Kantorovich, J. Magn. & Magn. Mater. **431**, 152 (2017).
40. H.J. Limbach, A. Arnold, B.A. Mann, C. Holm, Comput. Phys. Commun. **174**, 704 (2006).
41. J.J. Cerdà, V. Ballenegger, O. Lenz, C. Holm, J. Chem. Phys. **129**, 234104 (2008).
42. P.J. Steinhardt, D.R. Nelson, M. Ronchetti, Phys. Rev. B **28**, 784 (1983).
43. J. Bartke, R. Hentschke, Phys. Rev. E **75**, 061503 (2007).